Regional Comparison of Surface Turbulent Flux Products

Paul J. Hughes, **Shawn R. Smith**, and Mark A. Bourassa

Center for Ocean-Atmospheric Prediction Studies and Department of Meteorology

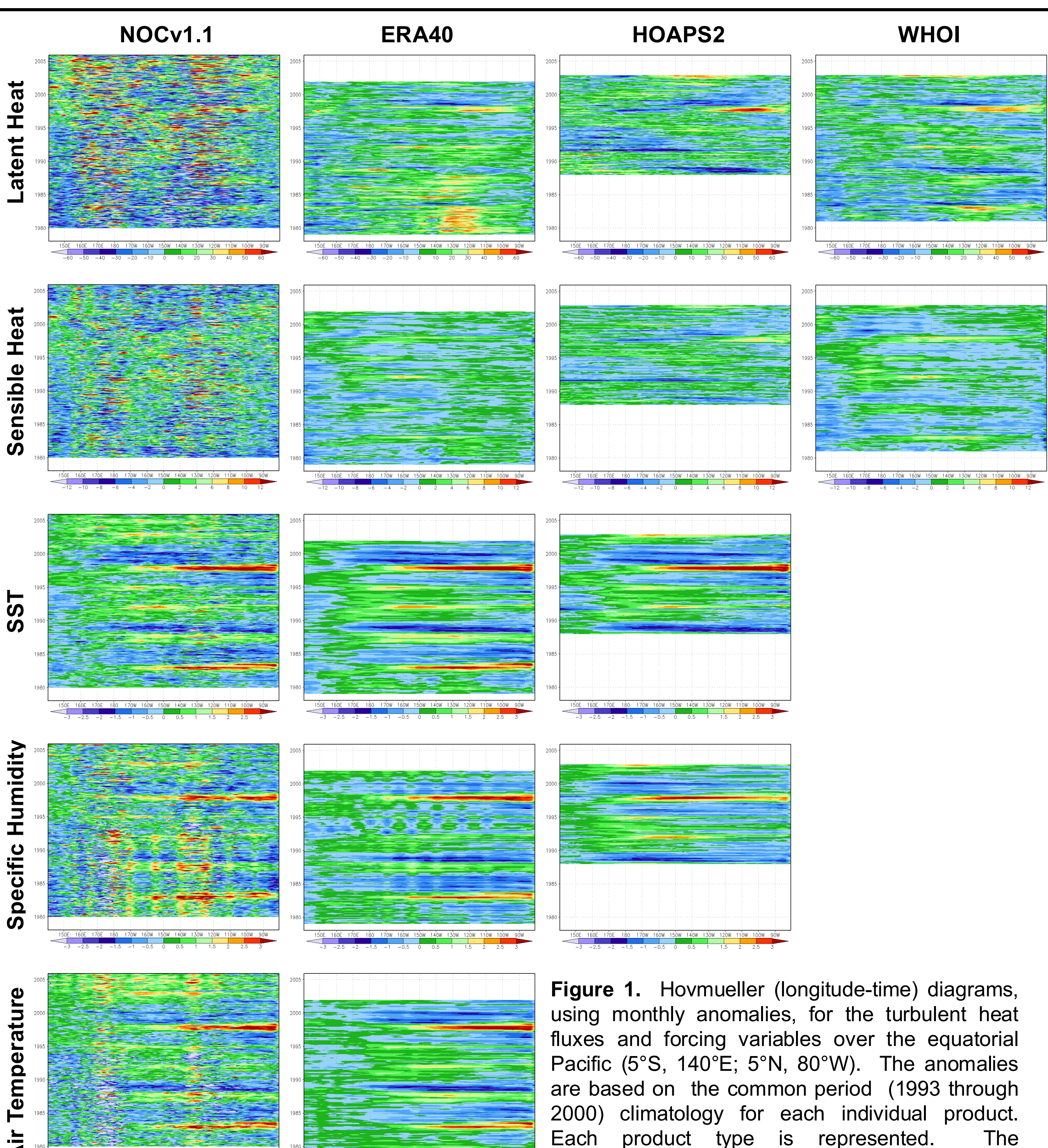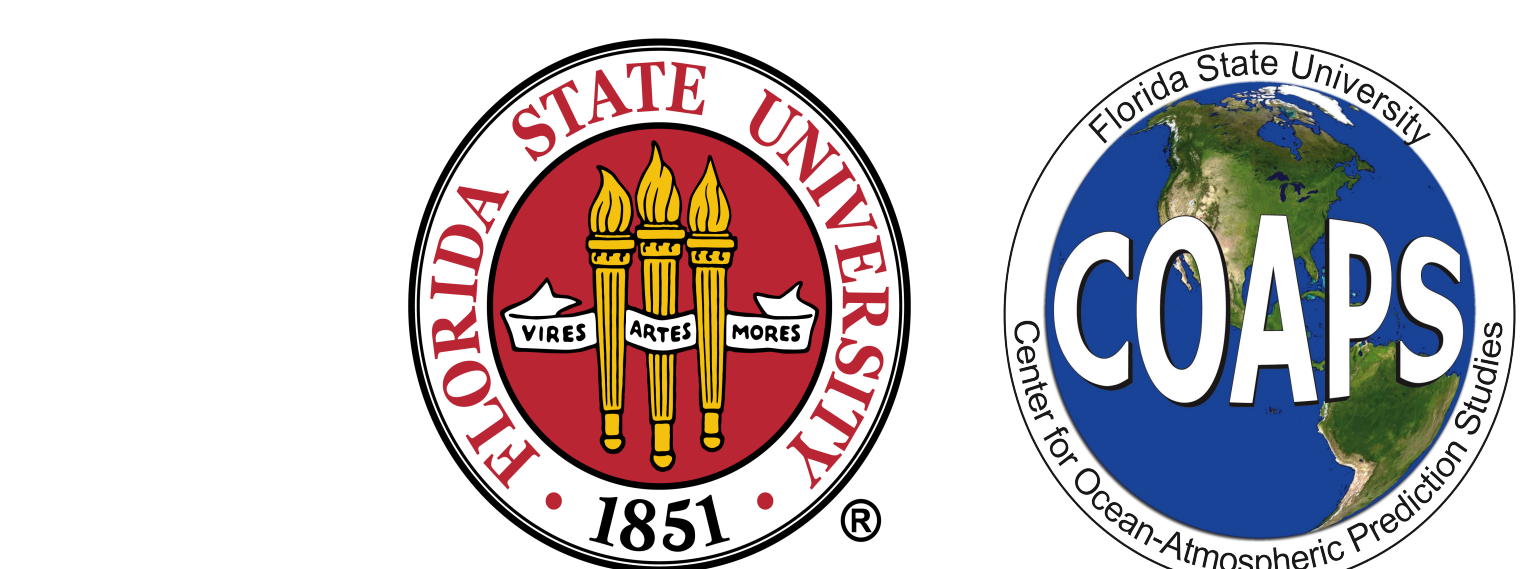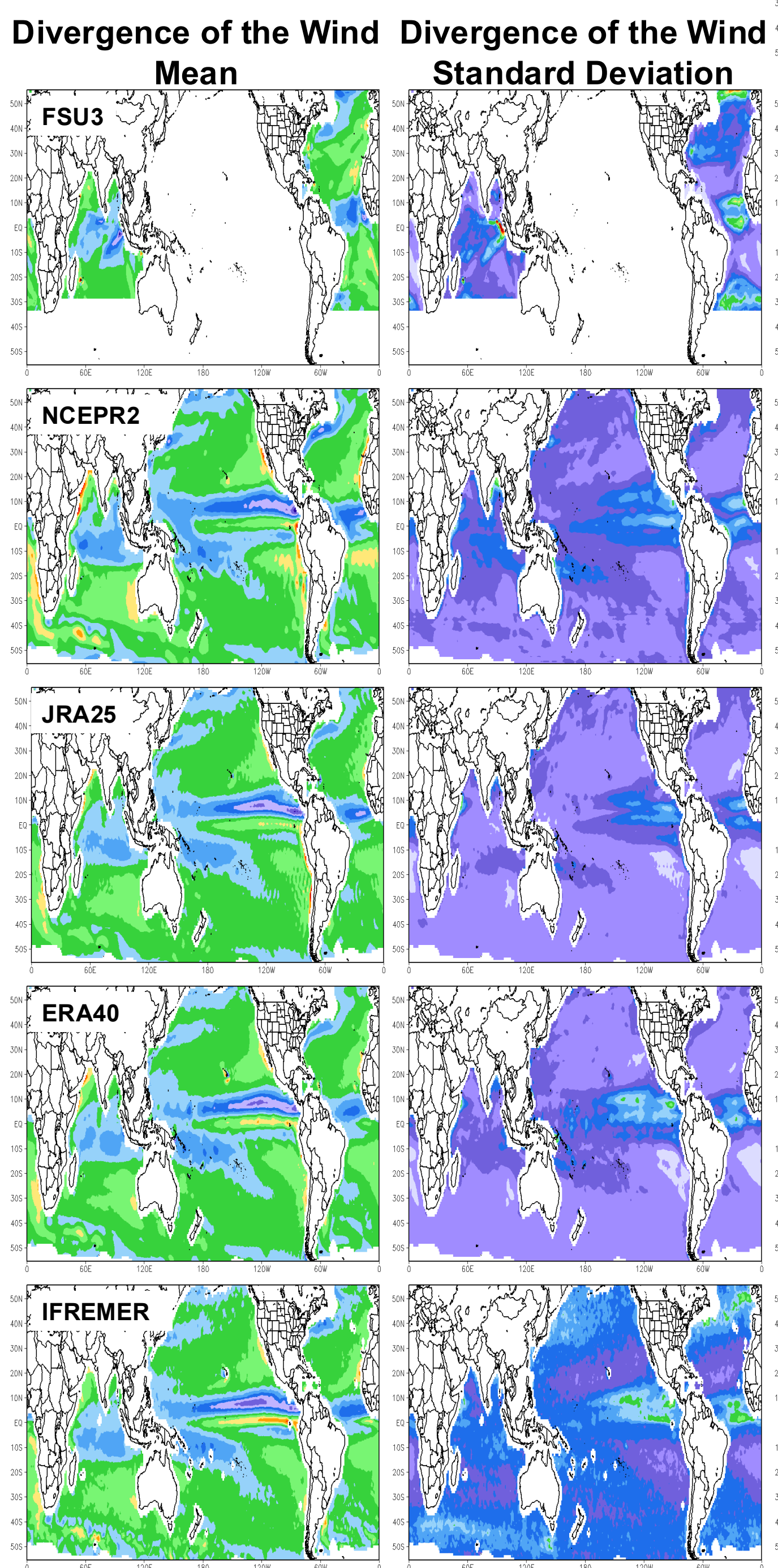Florida State University, Tallahassee, FL 32306-2840

phughes@met.fsu.edu

1. Introduction

Monthly averaged surface turbulent fluxes (stress, sensible heat, and latent heat) are compared for nine products. Reanalysis products include NCEPR2, JRA25, and ERA40. Satellite derived products include IFREMER and HOAPS2. Products based on ship and buoy observations include FSU3 and NOC1.1 (formerly SOC). Hybrid numerical weather prediction (NWP) model and satellite products include WHOI and GSSTF2. The common period of March 1993 through December 2000 is examined. Input data are also compared when available. Each product has been regridded onto a 1x1° grid. To reduce problems related to land, data within two grid cells of land are not used in this comparison.

2. Flux Product Information

There are many types of products that include turbulent fluxes of latent heat, sensible heat, and stress. Reanalysis products, created from NWP models with fixed model physics (albeit with changing data products for assimilation), are often used because of the spatiotemporal coverage and the additional information provided at various levels in the atmosphere. However, such models have poor representations of the atmospheric boundary layer, and questionable parameterizations of surface turbulent fluxes. Satellite derived products benefit from the much better sampling (small spatial and short temporal scales) of variables needed for air-sea flux calculations. However, the satellite derived fluxes are subject to uncertainties associated with the retrieval algorithms. Products based on ship and buoy observations provide a longer time series than the satellite based products (beneficial for climate studies), but suffer from poor/inhomogeneous sampling and uncertainties inherent in ship observations.

Product	LHF	SHF	Stress (x,y)	Wind Speed	u wind	v wind	Tair	Qair	SST	Product Type	Grid Spacing
NCEPR2	x	x			x	x	x	x	x	Reanalysis	Gaussian (T62, 194x94)
JRA25	x	x	x		x	x	x	x	x	Reanalysis	(T106L40) ~120km
ERA40	x	x	x		x	x	x	x	x	Reanalysis	1 1/8 degrees
WHOI	x	x								Hybrid	1 x 1 degree
GSSTF2	x	x	x	x				x		Hybrid	1 x 1 degree
IFREMER	x	x	x		x	x	x	x	x	Satellite	1 x 1 degree
HOAPS2	x	x	x				x	x	x	Satellite	0.5 x 0.5 degree
FSU3	x	x	x		x	x	x	x	x	In-situ	1 x 1 degree
NOC1.1	x	x	x				x	x		In-situ	1 x 1 degree

3. Discussion

Differences in the products can result from the input parameters and the methodology used to produce the turbulent flux fields (i.e., objective techniques and bulk flux algorithms). Figure 1 examines the similarity between the representation of physical processes (i.e., air-sea exchanges of latent and sensible heat associated with the El Nino – Southern Oscillation). Focusing on the common period, all of the products (except JRA and NOC) exhibit a discernable region of positive latent heat flux anomalies centered around 110°W associated with the 1997-98 El Nino. The satellite derived anomalies (HOAPS and IFREMER) have the largest spatial and temporal extent. Distinct negative anomalies coincide with the 1999-2000 La Nina in all products but NOC. Regarding sensible heat fluxes, all of the products (except NOC) show widespread positive (negative) anomalies associated with the aforementioned El Nino (La Nina) events, although the ERA40 positive anomalies are weaker. The most evident difference is the location of the positive anomalies. The satellite derived products (HOAPS and IFREMER) have the largest positive anomalies located farther eastward (centered around 105°W), coincident with smaller air temperature anomalies. This feature is also evident in the specific humidity, where the satellite products have smaller positive anomalies around 90°W. Figure 2 shows much variation between the latent and sensible heat fluxes at all quantiles in the equatorial Pacific, with JRA having drastically larger median values and lower variability.

The means of the turbulent heat fluxes and derived quantities (Figure 3) show similar patterns (except for the purely satellite derived sensible heat flux); however, the standard deviations reveal problems associated with objective techniques and the data assimilation. For example, the TAO buoy array is easily identified in the ERA40 and NOC products (including specific humidity and air temperature in figure 1). Ship tracks are seen in the FSU3 and NOC products. However, in the North Atlantic Ocean, where the ship coverage is much better, the ship tracks are not easily identified in the FSU3 fields. Other unrealistic features include the orographically induced ringing in the NCEPR2, JRA25, and GSSTF2 products.

These results are based on monthly averaged fluxes; therefore, they likely underestimate the issues with fluxes produced for shorter time scales. The large differences in fluxes, and in the spatial/temporal changes in these products indicate that there are still serious challenges to overcome in the construction of surface forcing fields for applications in climate and general oceanography.

4. Acknowledgements

Figure 1. Hovmueller (longitude-time) diagrams, using monthly anomalies, for the turbulent heat fluxes and forcing variables over the equatorial Pacific (5°S, 140°E; 5°N, 80°W). The anomalies are based on the common period (1993 through 2000) climatology for each individual product. Each product type is represented. The distributions of the turbulent fluxes and input variables for all available products in this region are shown in figure 2.
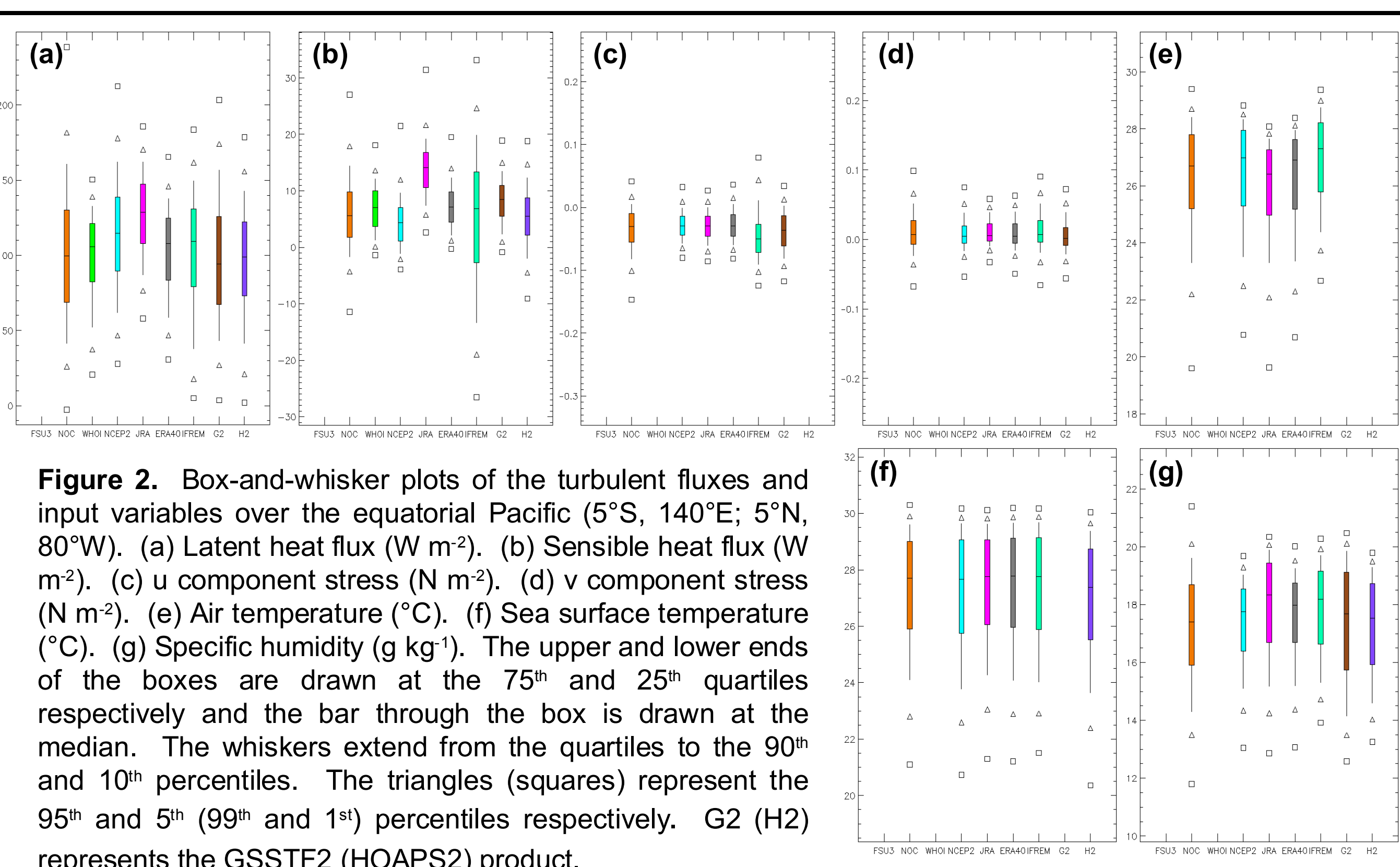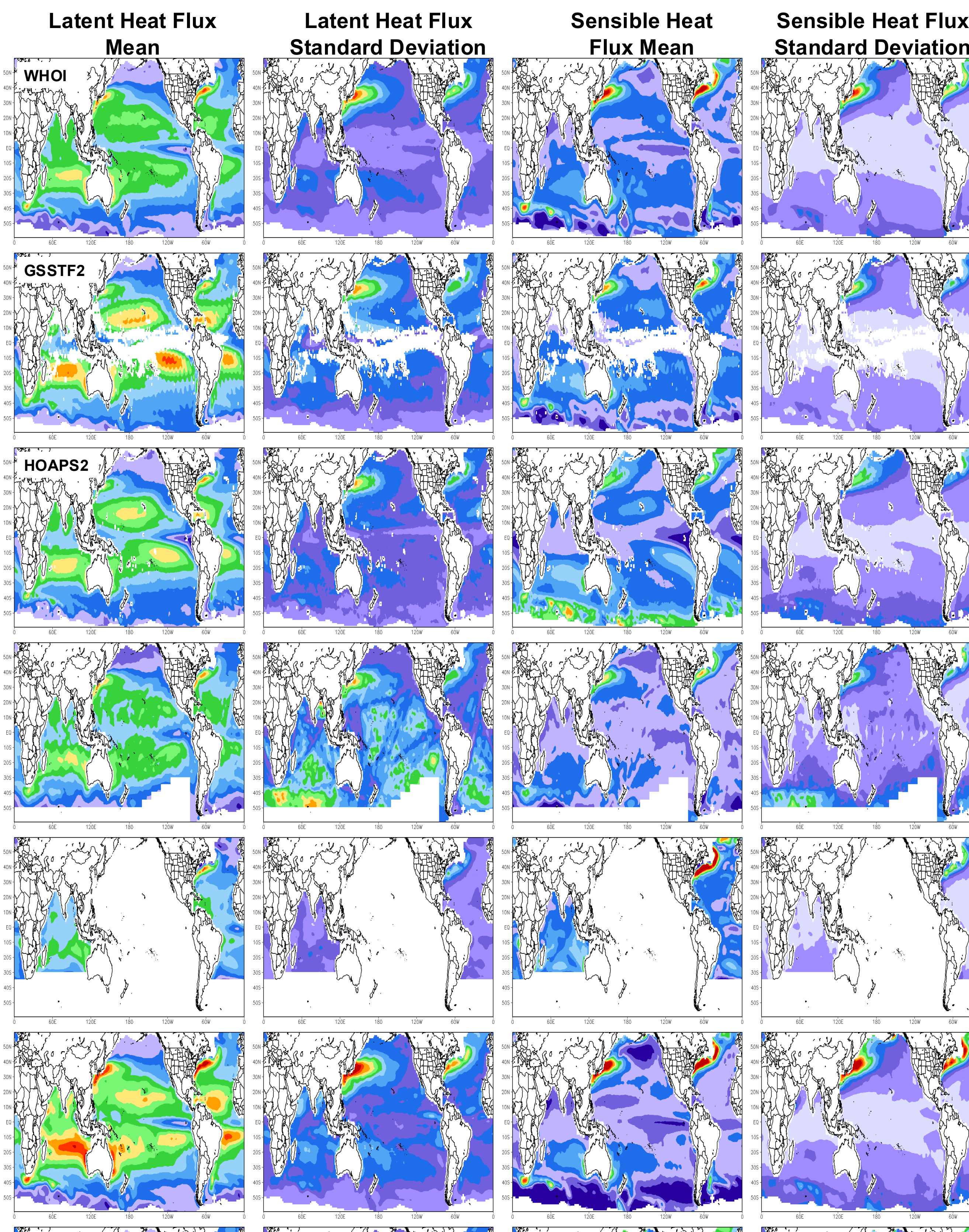

Figure 2. Box-and-whisker plots of the turbulent fluxes and input variables over the equatorial Pacific (5°S, 140°E; 5°N, 80°W). (a) Latent heat flux (W m⁻²). (b) Sensible heat flux (W m⁻²). (c) u component stress (N m⁻²). (d) v component stress (N m⁻²). (e) Air temperature (°C). (f) Sea surface temperature (°C). (g) Specific humidity (g kg⁻¹). The upper and lower ends of the boxes are drawn at the 75th and 25th quartiles respectively and the bar through the box is drawn at the median. The whiskers extend from the quartiles to the 90th and 10th percentiles. The triangles (squares) represent the 95th and 5th (99th and 1st) percentiles respectively. G2 (H2) represents the GSSTF2 (HOAPS2) product.

Figure 3. The mean and standard deviation are computed for the common period (March 1993 through December 2000). The curl of the wind stress is particularly important for ocean forcing; divergence of winds is important for atmospheric applications.